

# Approximate Loss and Delay Analysis of Two Priority Classes Sharing a Finite Buffer with GPS Scheduling \*

George D. Lapiotis<sup>1</sup>, Shivendra Panwar<sup>2</sup>  
Center for Advanced Technology in Telecommunications  
Polytechnic University  
6 Metrotech Center  
Brooklyn, NY 11201

November 3, 1997

## Abstract

In this paper we provide a new method to estimate the performance of two traffic streams which access a finite buffer using complete sharing, and share the capacity using the Generalized Processor Sharing scheduling policy. The input traffic is modeled by general Markov Modulated Fluid (MMF) sources. Specifically, approximate steady-state probability distributions for the content of the two logical queues are obtained and used to provide estimates of the loss probability and delay distribution of each session. Our approach is based on obtaining an initial estimate of the distributions in the region where the buffer and capacity resources are specifically allocated to each priority class and then refining this approximation by analyzing the effects on the boundaries. The techniques used can be applied to the infinite and finite queue cases, by using the appropriate boundary conditions in each case. This approach can be applied to service priority systems with GPS scheduling and admission policies assigning buffer space priority when the shared buffer is full. In this work we focus on the complete buffer sharing policy. We then show by means of examples that current call admission control methods can be greatly improved when using such priority schemes.

---

\*This research was supported by NYNEX Science and Technology, Inc., and the New York State Center for Advanced Technology in Telecommunications, Polytechnic University.

<sup>1,2</sup> Polytechnic University, Center for Advanced Technology in Telecommunications (CATT), 6 Metrotech Center, Brooklyn, NY 11201 (E-mail: {glapiot, panwar}@kanchi.poly.edu).

# 1 Introduction

The main objective in the future broadband integrated services network is the accommodation of a variety of services with different traffic characteristics and Quality of Service (QoS) requirements. This indicates that the network should provide special mechanisms in order to prioritize the access to resources, such as link capacity and buffer space. The allocation of resources is controlled using mechanisms such as call admission and policing, at the user-network interface, and scheduling at network nodes. For services with strict loss and/or delay requirements upon call admission the network must be able to reserve resources to guarantee the QoS of those services. As a general example, traditional data traffic (file transfer, e-mail) has strict loss requirement but is relatively insensitive to delay, while real-time traffic (video, voice) can tolerate some loss at the expense of strict delay requirements. Network nodes (switches, routers, etc) are being designed to accommodate at least these two types of priority classes. Most of the broadband switch architectures that have been proposed in the literature use some buffering to queue cells contending for the same switch output port. In a typical output buffered switch port, several traffic streams with different QoS requirements access a shared buffer according to a space priority scheme and bandwidth is shared using a scheduling algorithm. Currently, numerous packet scheduling algorithms used in high-speed switches aim at approximating the Generalized Processor Sharing (GPS) policy.

Generalized Processor Sharing (GPS) is a work conserving scheduling discipline in the which the  $n$  input sessions share a deterministic server with total rate  $c$ . A set of parameters  $\{\varphi_i\}_{1 \leq i \leq n}$ , called the GPS assignment, determine the share of service rate that each session receives as follows: the minimum service rate guaranteed to input session  $i$  is equal to  $c_i = \frac{\varphi_i}{\sum_{j=1}^n \varphi_j}$ . Also, the input traffic of session  $i$  is considered an infinitely divisible fluid that can be described by a continuous stochastic process  $r_i(t)$ . Thus, GPS can be considered a continuous limiting case of the Weighted Round Robin service discipline.

Most previous work on GPS analysis is mainly focused on very general arrival processes, with deterministic or stochastic settings. In [1, 2] the input process is described by Cruz's Linear Bounded Arrival Process (LBAP) model [3] with two parameters, a rate  $\rho$  and a maximum burst size  $\sigma$ ; at any time interval  $t$  the source traffic is bounded by  $\rho t + \sigma$ . In [4, 5] the source traffic is modelled by the Exponentially Bounded Burstiness (EBB) process [6]. Under both traffic model assumptions upper bounds on backlog and delay tail distributions are obtained. These results are general and are expected to give loose upper bounds of the distributions, because the dynamics of the arrival processes are not captured.

In [7] the sources are described by Markov Modulated Fluid Processes (MMFP), first introduced as network traffic sources in [10]. This source model has been shown to effectively model network traffic sources [8, 13]. The lower and upper bounds obtained in [7] for a two-queue GPS system,

are based on the approximation of the output process of a constant service queue fed by a MMFP, using spectral decomposition techniques first introduced in [11]. This approximation is based on an infinite buffer assumption and is not guaranteed to adequately model finite GPS buffer systems.

The contribution of this work is the development of an analytical method for a GPS system with both infinite and finite queue. We consider that the input traffic consists of two priority classes for simplicity. Analytical results provide a better understanding of the tradeoffs involved in sharing both buffer space and service capacity among sessions of a statistical multiplexer in work conserving systems with the flexibility and economy of bandwidth assignment that GPS offers. We are also able to evaluate the advantage of resource sharing in call admission control. The usual call admission control methods assume a fixed effective bandwidth for each source they are expected to be conservative (see the survey in [14] and the references therein). We show that for buffer regions of interest there is a significant margin for improvement, when a shared buffer GPS system is used. The analysis of the bounded buffer case assumes complete sharing of the buffer space between the two priority classes. However, with some additional effort, we believe that results can be extended to a larger class of buffer management schemes that control the space priority of the two traffic classes when the buffer is full. The case of multiple priority classes is an interesting open problem, under the MMF source traffic assumption.

The paper is organized as follows. In section 1 we formulate the problem and list the basic assumptions with two input multistate MMF sources with different QoS requirements sharing a buffer and using the GPS service policy. The general GPS scheduling problem with a finite queue is described in section 2. In section 3 we formulate the equations that describe the dynamics of the system and accordingly provide an approximate solution for the queue occupancy distribution for both the infinite and finite buffer case. In section 4 we compare analytical results with simulations. Additionally, to demonstrate the significant improvement in the capacity assignment of admission control methods, we compare the capacity requirement of the shared buffer GPS system, with the minimum capacity required by a fixed capacity allocation system. Section 5 contains conclusions and future work.

## 2 The General Model.

The problem formulation of buffer management using the GPS service policy can be described by the random processes of the input traffic streams, and the minimum capacity allocated to each of the logical queues in the buffer (GPS assignment). We consider two traffic streams each treated as a separate traffic class sharing a buffer of size  $B$ . Assume a time interval that one queue is empty and its instantaneous input rate is less than its guaranteed minimum service rate. During this time interval the other queue is assigned the residual service rate of the former queue in addi-

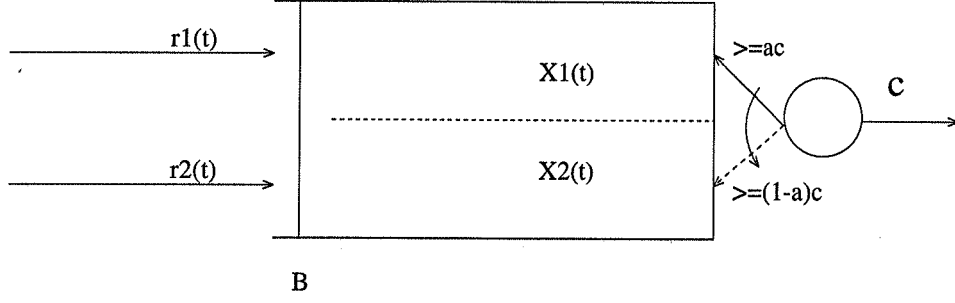


Figure 1: Bounded buffer with GPS service.

tion to its own guaranteed minimum service rate. The following modeling assumptions are made.

There are two input traffic streams described by the processes  $r_1(t)$ ,  $r_2(t)$  (see fig. 1), which in this work are two independent general Markov Modulated Fluid (MMF) sources characterized by the generator matrix  $\mathbf{A}$  and rate matrix  $\mathbf{\Lambda}$  for input  $r_1(t)$ , and the corresponding matrices  $\mathbf{B}$ ,  $\mathbf{M}$  for input  $r_2(t)$ , where

$$\mathbf{A} = \begin{bmatrix} -a_{11} & a_{12} & \cdots & a_{1N_1} \\ a_{21} & -a_{22} & \cdots & a_{2N_1} \\ \cdot & \cdot & \cdot & \cdot \\ \cdot & \cdot & \cdot & \cdot \\ \cdot & \cdot & \cdot & \cdot \\ a_{N_11} & a_{N_12} & \cdots & -a_{N_1N_1} \end{bmatrix}, \quad \mathbf{B} = \begin{bmatrix} -b_{11} & b_{12} & \cdots & b_{1N_2} \\ b_{21} & -b_{22} & \cdots & b_{2N_2} \\ \cdot & \cdot & \cdot & \cdot \\ \cdot & \cdot & \cdot & \cdot \\ \cdot & \cdot & \cdot & \cdot \\ b_{N_21} & b_{N_22} & \cdots & -b_{N_2N_2} \end{bmatrix},$$

$$\mathbf{\Lambda} = \text{diag}\{\lambda_1, \lambda_2, \dots, \lambda_{N_1}\}, \quad \mathbf{M} = \text{diag}\{\mu_1, \mu_2, \dots, \mu_{N_2}\}.$$

In the above, the assumption is made that traffic source 1 (2) has  $N_1$  ( $N_2$ ) states. Also,  $\lambda_l$  is the arrival rate when the source 1 rate process is in state  $S_1(t) = l$ , and  $\mu_m$  is the arrival rate when the source 2 rate process is in state  $S_2(t) = m$ . The combined total arrival rate of the two sessions can be described by a global  $K$ -state MMF process ( $K = N_1N_2$ ) whose state at time  $t$  is  $S(t) \stackrel{\text{def}}{=} (S_1(t), S_2(t)) \in \mathcal{G}$ , where  $\mathcal{G} = \{(i, j) : i = 0, 1, \dots, N_1 - 1; j = 0, 1, 2, \dots, N_2 - 1\}$ . The set of pairs in  $\mathcal{G}$  are ordered lexicographically. Let  $k = S(t) = (i, j)$ , where  $k \in \{1, \dots, K\}$ , denote the  $k$ -th ordered pair on  $\mathcal{G}$ . The stationary probability distribution of process  $r_i(t)$  is denoted by the column vector  $\pi_i$ , where

$$\pi_i = [\pi_{i1}, \pi_{i2}, \dots, \pi_{iN_i}]^T, \quad i = 1, 2. \quad (1)$$

Then,  $\mathbf{A}^T \pi_1 = 0$ , and  $\mathbf{B}^T \pi_2 = 0$ , where the superscript  $T$  denotes the transpose of a matrix. The generator matrix  $\mathbf{G}$  and the stationary vector probability vector  $\pi$  of the global system arrival process are respectively given by,

$$\mathbf{G} = \mathbf{A}^T \oplus \mathbf{B}^T, \quad \text{and} \quad \pi = \pi_1 \otimes \pi_2. \quad (2)$$

The operators “ $\otimes$ ”, “ $\oplus$ ” denote the Kronecker product and sum, respectively. The total system has an output server of rate  $c$ . The minimum guaranteed service fraction for class 1 is  $a$ , and for class 2 is  $1-a$ . The transmission capacity allocated to each of the two traffic streams is described by the processes  $C_1(t)$  and  $C_2(t)$  where

$$C_1(t) = \begin{cases} c, & \text{if } X_2(t) = 0 \\ c_1 = ac, & \text{if } X_2(t) > 0 \end{cases}, \quad C_2(t) = \begin{cases} c, & \text{if } X_1(t) = 0 \\ c_2 = (1-a)c, & \text{if } X_1(t) > 0 \end{cases}. \quad (3)$$

By  $X_i(t)$  we denote the content of class  $i$  logical queue at time  $t$ , and by  $c_i$  the minimum guaranteed service rate for class  $i$ , where  $i = \{1, 2\}$ . The instantaneous drift rate for the content of logical queue  $i$  is given by  $d_i(t) \equiv dX_i(t)/dt$ , where

$$\begin{aligned} \frac{d}{dt}X_1(t) &= r_1(t) - \{ac + [(1-a)c - r_2(t)]^+ \mathbf{1}_{\{X_2(t)=0\}}\}, \quad \text{for } X_1(t) > 0 \\ \frac{d}{dt}X_2(t) &= r_2(t) - \{(1-a)c + [ac - r_1(t)]^+ \mathbf{1}_{\{X_1(t)=0\}}\}, \quad \text{for } X_2(t) > 0, \end{aligned} \quad (4)$$

where “ $\mathbf{1}_{\Omega}$ ” is the indicator function, and  $(x-y)^+ = \max\{x-y, 0\}$ . Each of the drift equations (2) includes two cases depending on the buffer content of the other queue. Table 1 contains all four cases.

Queue	Condition	Drift at source state (i,j)
1	$0 < X_1(t)$ and $X_2(t) = 0$	$d_1(i, j) = \lambda_i + \mu_j - c$
1	$0 < X_1(t)$ and $X_2(t) > 0$	$d_1(i, j) = \lambda_i - c_1$
2	$0 < X_2(t)$ and $X_1(t) = 0$	$d_2(i, j) = \lambda_i + \mu_j - c$
2	$0 < X_2(t)$ and $X_1(t) > 0$	$d_2(i, j) = \mu_j - c_2$

Table 1: Drift Cases

In the general model of fig.(1) the buffer is finite, which raises the issue of buffer space allocation between the two traffic classes. A discarding policy can be used in order to prioritize access to the buffer, when it is full. In this work we assume a complete sharing buffer access policy. Both session’s customers are dropped when the shared queue is full upon their arrival. Observe also that in the asymptotic case, i.e. as  $B \rightarrow \infty$ , the problem reduces to that of two separate buffers or logical queues, one for each input stream, which share the available service capacity according to the GPS scheme.

### 3 System Equations

We next derive the differential equations that govern the dynamics of the system. Define first the joint probability distribution functions

$$P_{ij}^W(t, x_1, x_2) \equiv \Pr\{S(t) = (i, j); X_1(t) \leq x_1, X_2(t) \leq x_2, t\}, x_1 > 0, x_2 > 0, \quad (5)$$

where  $S(t)$  denotes the global source state of the two independent arrival processes  $r_1(t), r_2(t)$ . For example, in the simple case of two-state MMF sources (on-off sources)  $r_1(t), r_2(t)$  can be in one of two states 0 or 1, i.e. for any  $t$ ,  $r_1(t), r_2(t) \in \{0, 1\}$ , and  $S(t) = (r_1(t), r_2(t)) \in \mathcal{G} = \{(0, 0), (0, 1), (1, 0), (1, 1)\}$ . Since the drift rates of  $X_1(t)$  and  $X_2(t)$  change on the boundaries  $x_2 = 0$  and  $x_1 = 0$ , respectively, (see table 1), we also need to define separately the joint pdf-s restricted on and beyond those boundaries as follows:

For  $X_1(t)$ ,

$$P_{ij}^{10}(t, x_1) \equiv \Pr\{S(t) = (i, j); X_1(t) \leq x_1, X_2(t) = 0, t\}, x_1 \geq 0, \quad (6)$$

$$P_{ij}^{11}(t, x_1) \equiv \Pr\{S(t) = (i, j); X_1(t) \leq x_1, X_2(t) > 0, t\}, x_1 \geq 0, \quad (7)$$

and for  $X_2(t)$ ,

$$P_{ij}^{20}(t, x_2) \equiv \Pr\{S(t) = (i, j); X_2(t) \leq x_2, X_1(t) = 0, t\}, x_2 \geq 0, \quad (8)$$

$$P_{ij}^{21}(t, x_2) \equiv \Pr\{S(t) = (i, j); X_2(t) \leq x_2, X_1(t) > 0, t\}, x_2 \geq 0, \quad (9)$$

where in the superscript of  $P^{kl}$ ,  $k$  denotes the queue content that is variable in the restricted joint pdf, and  $l$  is either 0, if the restricted queue is equal to 0, or 1, if the restricted queue is greater than 0. Define at steady state,

$$F_{ij}^S \equiv \lim_{t \rightarrow \infty} P_{ij}^S(t, x_1, x_2), \quad \text{for all superscripts } S \text{ in definitions (5)-(9)}. \quad (10)$$

In the area W of fig.(2)),  $x_1 > 0, x_2 > 0$  (the area W is infinite as  $B \rightarrow \infty$ ), the queues do not interact, since each queue receives only its minimum guaranteed service rate. In this case the system is described by a system of partial differential equations (pde-s), which can be derived as in [9]. Let

$$\mathbf{F}^W(x_1, x_2) = [F_{00}^W(x_1, x_2), F_{01}^W(x_1, x_2), \dots, F_{0(N_2-1)}^W(x_1, x_2), \dots, \\ F_{(N_1-1)0}^W, \dots, F_{(N_1-1)1}^W(x_1, x_2), F_{(N_1-1)(N_2-1)}^W(x_1, x_2)]^T.$$

Then, the pde system is the following:

$$[\Delta_1 \otimes \mathbf{I}] \frac{\partial \mathbf{F}^W(x_1, x_2)}{\partial x_1} + [\mathbf{I} \otimes \Delta_2] \frac{\partial \mathbf{F}^W(x_1, x_2)}{\partial x_2} = (\mathbf{A}^T \oplus \mathbf{B}^T) \mathbf{F}^W(x_1, x_2), x_1 > 0, x_2 > 0, \quad (11)$$

where  $\Delta_1, \Delta_2$  are the diagonal drift matrices defined as,

$$\Delta_1 = \Lambda - c_1 I, \quad \Delta_2 = M - c_2 I, \quad (12)$$

$I$  is the identity matrix appropriately dimensioned for each case. We next consider the restricted joint distributions  $F_{ij}^{10}(x_1), F_{ij}^{20}(x_2)$ . Along each of the boundaries  $x_1 = 0$  and  $x_2 = 0$  (see fig. (2)), the logical queues 2 and 1, respectively, receive full service. Along the boundary  $x_2 = 0$  we must not consider source states  $(i, j)$  in which  $\mu_j > c_2$ , since in those states  $X_2(t)$  cannot be zero. Therefore, we need only consider the state space of the underflow states of session 2, denoted by  $U_2 = \{(i, j) : \mu_j < c_2\}$ . Similarly, along the boundary  $x_1 = 0$  we need only consider the underflow states of session 1, i.e. the set  $U_1 = \{(i, j) : \lambda_i < c_1\}$ . The difference equations that describe the system along the  $x_1$  axis for  $x_1 \geq 0$  are,

$$\begin{aligned} P_{ij}^{10}(t + \delta t, x_1) &= (1 - a_{ii})(1 - b_{ii})P_{ij}^{10}(t, x_1 - (\lambda_i - c_1)\delta t) \\ &+ \sum_{l \neq i} P_{lj}^{10}(t, x_1) a_{li} \delta t (1 - b_{jj} \delta t) + \sum_{k \neq j} P_{ik}^{10}(t, x_1) (1 - a_{ii} \delta t) b_{kj} \delta t \\ &+ (1 - a_{ii})(1 - b_{ii})P_{ij}^W(t, x_1, 0 < X_2(t) \leq C_2(X_1)\delta t) \end{aligned} \quad (13)$$

The last additive term in eq.(13) represents the system transitions from the strip  $S$  in fig.(2) to the boundary  $x_2 = 0$ . By rearranging terms, dividing by  $\delta t$  and passing to the limits  $\delta t \rightarrow 0$ , and  $t \rightarrow \infty$  we obtain a system of ordinary differential equations (ode-s) for the equilibrium distributions  $F_{ij}^{10}(x_1) = \lim_{t \rightarrow \infty} P_{ij}^{10}(t, x_1), (i, j) \in U_2$ ,

$$\begin{aligned} (\lambda_i - c) \frac{d}{dx_1} F_{ij}^{10}(x_1) &= -(a_{ii} + b_{jj})F_{ij}^{10}(x_1) + \sum_{l \neq i} a_{li} F_{lj}^{10}(x_1) + \sum_{k \neq j} b_{kj} F_{ik}^{10}(x_1) \\ &+ \lim_{\delta t \rightarrow 0} \frac{P_{ij}^W(x_1, 0 < X_2(t) \leq C_2(X_1)\delta t)}{\delta t} \end{aligned} \quad (14)$$

Note that the additive terms on the right side of (14) require the solution of (11), which in turn is bounded by the  $x_1$ -axis on which (14) holds. As an example, in the case of two-state MMF sources for both input streams, (14) becomes,

$$\left\{ \begin{aligned} (-c) \frac{d}{dx_1} F_{00}^{10}(x_1) &= -(a_1 + b_1)F_{00}^{10}(x_1) + a_2 F_{10}^{10}(x_1) + \lim_{\delta t \rightarrow 0} \frac{P_{00}^W(x_1, 0 < X_2(t) \leq C_2(X_1)\delta t)}{\delta t} \\ (\lambda_1 - c) \frac{d}{dx_1} F_{10}^{10}(x_1) &= a_1 F_{00}^{10}(x_1) - (a_2 + b_1)F_{10}^{10}(x_1) + \lim_{\delta t \rightarrow 0} \frac{P_{10}^W(x_1, 0 < X_2(t) \leq C_2(X_1)\delta t)}{\delta t} \end{aligned} \right. \quad (15)$$

A similar system of ode-s holds along the  $x_1 = 0$  boundary. The overall queueing system solution requires solving the pde system (11), using as boundary conditions the ode system (15) on the

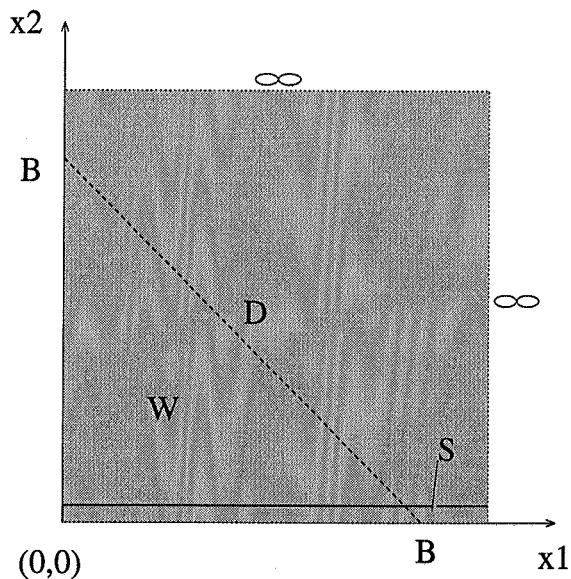


Figure 2: Derivation of system equations.

$x_2 = 0$  line, and the corresponding ode system on the  $x_1 = 0$  line, as well as boundary conditions at  $(0,0)$  and either at infinity for the infinite queue system or on the boundary  $D$ , where  $x_1 + x_2 = B$ , for the finite queue system. The exact closed-form solution of (11) is difficult to obtain because of its form, as well as because of its coupling with the boundary systems of ode-s. In the next section we describe a technique to approximate the system solution, that can be applied to the infinite and finite queue assumption, by applying appropriate boundary conditions in each case.

### 3.1 Solution of Joint Distribution in the Area $W$

As a first step, we proceed with an approximate solution of the problem in area  $W$ , with an initial assumption that in this area the variables  $X_1(t)$  and  $X_2(t)$  are independent and their joint distribution can be expressed as,

$$\mathbf{F}^W(x_1, x_2) = \mathbf{F}_1^W(x_1) \otimes \mathbf{F}_2^W(x_2), \quad (16)$$

where  $\mathbf{F}_i(x_i)$  is the steady state vector distribution function of  $X_i(t)$ ,  $i \in \{1, 2\}$ . This approximate joint distribution is expected to become more accurate for large  $B$ , and is only used to derive an estimate of the additive limiting terms in (14). In a second step of the analysis, in which the interaction between  $X_1(t)$  and  $X_2(t)$  is explicitly taken into account, this system is solved to obtain  $\mathbf{F}^{10}(x_1)$ , that is the distribution of  $X_1(t)$  along the line  $x_2 = 0$ . Similarly, we can obtain  $\mathbf{F}^{20}(x_2)$ . To determine  $\mathbf{F}_i^W(x_i)$  we observe that the two independent systems can be characterized



by the two sets of ode-s (see also [10]),

$$\Delta_1 \frac{d}{dx_1} \mathbf{F}_1^W = \mathbf{A} \mathbf{F}_1^W, \quad \Delta_2 \frac{d}{dx_2} \mathbf{F}_2^W = \mathbf{B} \mathbf{F}_2^W, \quad (17)$$

where the matrices  $\mathbf{A}$ ,  $\mathbf{B}$ ,  $\Delta_1$ ,  $\Delta_2$  were defined in section 2. The solution of (17) is obtained by first extracting the eigenpairs  $(\nu, \varphi)$  and  $(\mu, \psi)$  of the corresponding eigensystems

$$\nu \Delta_1 \varphi = \mathbf{A} \varphi, \quad \mu \Delta_2 \psi = \mathbf{B} \psi. \quad (18)$$

Then the solution of eqs. (17) has the form

$$\mathbf{F}_1^W(x_1) = \sum_m a_m e^{\nu_m x_1} \varphi_m, \quad \mathbf{F}_2^W(x_2) = \sum_k b_k e^{\mu_k x_2} \psi_k, \quad (19)$$

where  $\nu_m, \mu_k$  are eigenvalues,  $\varphi_m, \psi_k$  are the corresponding eigenvectors, and  $a_m, b_k$  are coefficients to be determined from the boundary conditions at 0 and either  $\infty$  in the infinite buffer case, or along the boundary D in the finite buffer case. Therefore the joint pdf in (16) can be further expressed as:

$$\mathbf{F}^W(x_1, x_2) = \sum_m \sum_k \alpha_{mk} e^{\nu_m x_1} e^{\mu_k x_2} (\varphi_m \otimes \psi_k). \quad (20)$$

In (20) we represent the product terms  $a_m b_k$  of (19) by  $\alpha_{mk}$ . In the infinite buffer case boundary conditions for the two logical queues can be independently applied to each one's distribution in (19), since the system is equivalent to one of two independent queues with no boundary [10]. In the finite buffer case the joint distribution is normalized in the triangular area defined by the points  $(0, 0)$ ,  $(0, B)$ , and  $(B, 0)$ , as in [9]. Next, consider the limiting additive terms in both equations of system (15), which can be written as,

$$\forall x_1 \geq 0,$$

$$\lim_{\delta t \rightarrow 0} \frac{1}{\delta t} P_{ij}^W(X_1(t) \leq x_1, 0 < X_2(t) \leq C_2(X_1)\delta t) \quad (21)$$

$$= \lim_{\delta t \rightarrow 0} \frac{1}{\delta t} [P_{ij}^W(X_1(t) \leq 0, 0 < X_2(t) \leq c\delta t) + P_{ij}^W(0 < X_1(t) \leq x_1, 0 < X_2(t) \leq c_2\delta t)] \quad (22)$$

$$= \lim_{\delta t \rightarrow 0} \left[ \frac{F_{ij}^W(0, c\delta t) - F_{ij}^W(0, 0)}{\delta t} \right] + \lim_{\delta t \rightarrow 0} \left[ \frac{F_{ij}^W(x_1, c_2\delta t) - F_{ij}^W(x_1, 0)}{\delta t} \right] \\ - \lim_{\delta t \rightarrow 0} \left[ \frac{F_{ij}^W(0, c_2\delta t) - F_{ij}^W(0, 0)}{\delta t} \right], \quad (23)$$

where (23) results by applying the properties of joint distribution functions on (22). From (20) the components of  $\mathbf{F}^W(x_1, x_2)$  are

$$F_{ij}^W(x_1, x_2) = \sum_m \sum_k \alpha_{mk} e^{\nu_m x_1} e^{\mu_k x_2} \varphi_{im} \psi_{jk}. \quad (24)$$

We note that in the eigenvector components  $\varphi_{im}$ ,  $\psi_{jk}$  above, the first indices  $i$  and  $j$  denote the order of the component in the  $m$ -th and  $k$ -th eigenvector, respectively. Substituting (24) in (23) we get:

$$\begin{aligned}
& \lim_{\delta t \rightarrow 0} \frac{\sum_m \sum_k \alpha_{mk} \varphi_{im} \psi_{jk} (e^{\mu_k c \delta t} - 1)}{\delta t} + \lim_{\delta t \rightarrow 0} \frac{\sum_m \sum_k \alpha_{mk} \varphi_{im} \psi_{jk} e^{\nu_m x_1} (e^{\mu_k c_2 \delta t} - 1)}{\delta t} \\
& - \lim_{\delta t \rightarrow 0} \frac{\sum_m \sum_k \alpha_{mk} \varphi_{im} \psi_{jk} (e^{\mu_k c_2 \delta t} - 1)}{\delta t} \\
& = \sum_m \sum_k \alpha_{mk} \varphi_{im} \psi_{jk} \mu_k c + \sum_m \sum_k \alpha_{mk} \varphi_{im} \psi_{jk} e^{\nu_m x_1} \mu_k c_2 \\
& - \sum_m \sum_k \alpha_{mk} \varphi_{im} \psi_{jk} \mu_k c_2 \\
& = \sum_m \sum_k \alpha_{mk} \varphi_{im} \psi_{jk} \mu_k c_2 e^{\nu_m x_1} + \sum_m \sum_k \alpha_{mk} \varphi_{im} \psi_{jk} \mu_k (c - c_2). \tag{25}
\end{aligned}$$

Define,

$$\hat{\theta}_{ij}(x_1) = \theta_{ij}(x_1) + k_{ij}, \tag{26}$$

where  $\theta_{ij}(x_1)$  is the first and  $k_{ij}$  the second term on the right of (25), respectively.

### 3.2 Derivation of Boundary Distribution $\mathbf{F}^{10}(x_1)$

System (14) can now be re-written in the following matrix form:

$$\mathbf{D}_1 \frac{d}{dx_1} \mathbf{F}^{10}(x_1) = \mathbf{G}^* \mathbf{F}^{10}(x_1) + \hat{\Theta}(x_1), \tag{27}$$

where  $\mathbf{D}_1$  is the diagonal drift matrix with diagonal elements

$$D_1(i, j) = \lambda_i + \mu_j - c, \quad (i, j) \in U_2, \tag{28}$$

$\mathbf{G}$  is the global source generator, and the superscript  $*$  denotes deletion of rows and columns in the original matrix that correspond to states that do not belong in  $U_2$ , the set of underflow source states of the MMF source of session 2, Accordingly the vector  $\mathbf{F}^{10}(x_1)$  in this system does not include the components corresponding to states  $(i, j) \notin U_2$ , since those components are equal to zero. The additive vector  $\hat{\Theta}(x_1)$  has components  $\hat{\theta}_{ij}(x_1)$ , for  $(i, j) \notin U_2$ , as defined in (26). The system (27) is a nonhomogeneous linear ode system. To solve we first transform the ode system to its canonical form. Let  $\mathbf{T}$  be the matrix whose columns are the eigenvectors of  $\mathbf{D}_1^{-1} \mathbf{G}^*$ , and define the transformation

$$\mathbf{F}^{10} = \mathbf{T} \mathbf{Y}. \tag{29}$$

By substituting for  $\mathbf{F}^{10}$  in (27) we obtain the transformed system in the canonical form

$$\mathbf{Y}'(x_1) = (\mathbf{T}^{-1}\mathbf{D}_1^{-1}\mathbf{G}^*\mathbf{T})\mathbf{Y}(x_1) + (\mathbf{T}^{-1}\mathbf{D}_1^{-1})\hat{\mathbf{G}}(x_1) = \mathbf{R}\mathbf{Y}(x_1) + \mathbf{H}(x_1), \quad (30)$$

where

$$\mathbf{R} = \mathbf{T}^{-1}\mathbf{D}_1^{-1}\mathbf{G}^*\mathbf{T}, \quad \text{and } \mathbf{H}(x_1) = \mathbf{T}^{-1}\mathbf{D}_1^{-1}\hat{\mathbf{G}}(x_1) \quad (31)$$

The matrix  $\mathbf{R}$  is by construction diagonal with entries the eigenvalues of  $\mathbf{D}_1^{-1}\mathbf{G}^*$ , so that (30) is a system of uncoupled first order linear equations with solutions of the form

$$y_\sigma = c_\sigma e^{r_\sigma x_1} + e^{r_\sigma x_1} \int_0^{x_1} e^{-r_\sigma x} h_\sigma(x) dx, \quad (32)$$

where  $c_\sigma$  are coefficients to be derived from boundary conditions,  $r_\sigma$  are eigenvalues of  $\mathbf{D}_1^{-1}\mathbf{G}^*$ , and  $h_\sigma(x_1)$  the components of  $\mathbf{H}(x_1)$ . From the second definition of (31)  $h_\sigma(x_1)$  can be expressed as a linear combination of  $\hat{\theta}_{ij}(x_1)$ , i.e.,

$$h_\sigma(x_1) = \sum_{\mu} \delta_{\sigma\mu} \hat{\theta}_{\mu}(x_1), \quad (33)$$

where  $\delta_{\sigma\mu}$  are the elements of  $\mathbf{T}^{-1}\mathbf{D}_1^{-1}$  and we let the indices  $\mu$ ,  $\sigma$ , and  $l$  denote the lexicographical order of the global state indices  $(i, j) \in U_2$ . Furthermore, from transformation (29) we can obtain the components  $F_l^{10}(x_1)$  of  $\mathbf{F}^{10}$  as

$$F_l^{10}(x_1) = \sum_{\sigma} \tau_{l\sigma} y_{\sigma}, \quad (34)$$

where  $\tau_{l\sigma}$  are the elements of  $\mathbf{T}$ . Accordingly, substituting for  $y_{\sigma}$  and  $h_{\sigma}$ ,

$$\begin{aligned} F_l^{10}(x_1) &= \sum_{\sigma} \tau_{l\sigma} \left\{ c_{\sigma} e^{r_{\sigma} x_1} + e^{r_{\sigma} x_1} \int_0^{x_1} e^{-r_{\sigma} x} \left[ \sum_{\mu} \delta_{\sigma\mu} \hat{\theta}_{\mu}(x) \right] dx \right\} \\ &= \sum_{\sigma} c_{\sigma} \tau_{l\sigma} e^{r_{\sigma} x_1} + \sum_{\sigma} \sum_{\mu} \tau_{l\sigma} \delta_{\sigma\mu} e^{r_{\sigma} x_1} u_{\sigma\mu}(x_1), \end{aligned} \quad (35)$$

where

$$u_{\sigma\mu}(x_1) = \int_0^{x_1} e^{-r_{\sigma} x} \hat{\theta}_{\mu}(x) dx. \quad (36)$$

Using the definition of  $\hat{\theta}_{\mu}(x)$  from (26) we get

$$u_{\sigma\mu}(x_1) = \sum_m \sum_k a_{mk} \varphi_{\mu m} \psi_{0k} \mu_k \frac{c_2}{\nu_m - r_{\sigma}} \left[ e^{(\nu_m - r_{\sigma}) x_1} - 1 \right] \quad (37)$$

The first term on the right is the general solution of the homogeneous system (27) and the second term is a particular solution. From eqs. (35)-(37) we obtain the general solution

$$F_l^{10}(x_1) = \sum_{\sigma} c_{\sigma} \tau_{l\sigma} e^{r_{\sigma} x_1} + \sum_{\sigma} \sum_{\mu} \tau_{l\sigma} \delta_{\sigma\mu} u_{\sigma\mu}(x_1), \quad (38)$$

where,  $\tau_{\sigma}$  are the eigenvectors of  $\mathbf{D}_1^{-1} \mathbf{G}^*$ , and

$$\begin{aligned} u_{\sigma\mu}(x_1) &= e^{r_{\sigma} x_1} u_{\sigma\mu}(x_1) \\ &= \sum_m \sum_k a_{mk} \varphi_{im} \psi_{jk} \mu_k \frac{c_2}{\nu_m - r_{\sigma}} [e^{\nu_m x_1} - e^{r_{\sigma} x_1}] \end{aligned} \quad (39)$$

The form of  $u_{\sigma\mu}(x_1)$  in (39) implies that by re-grouping the general solution (38) can be written as,

$$F_l^{10}(x_1) = \sum_{\sigma} \bar{c}_{\sigma} \tau_{l\sigma} e^{r_{\sigma} x_1} + \sum_{\sigma} \sum_{\mu} \tau_{l\sigma} \delta_{\sigma\mu} \hat{u}_{\sigma\mu}(x_1), \quad (40)$$

where

$$\bar{c}_{\sigma} = c_{\sigma} - \sum_{\mu} \tau_{l\sigma} \delta_{\sigma\mu} \sum_m \sum_k a_{mk} \varphi_{im} \psi_{jk} \mu_k \frac{c_2}{\nu_m - r_{\sigma}} \quad (41)$$

and,

$$\hat{u}_{\sigma\mu}(x_1) = \sum_m \sum_k a_{mk} \varphi_{im} \psi_{jk} \mu_k \frac{c_2}{\nu_m - r_{\sigma}} e^{\nu_m x_1} \quad (42)$$

It remains to obtain the coefficients  $\bar{c}_{\sigma}$  using boundary conditions.

### 3.3 Boundary Conditions for $F^{10}(x_1)$

#### I. Infinite buffer case

In (40) the coefficients  $\bar{c}_{\sigma}$  from a linear system of equations that results by applying the conditions at the boundaries  $x_1 = 0$  and  $x_1 = \infty$ . At the point  $x_1 = 0$  for all states such that the drift  $d_1(i, j)$  is positive, i.e. for all overflow states  $(i, j)$ , the probability of empty queue 1 becomes zero:

$$F_l^{10}(x_1 = 0) = 0, \forall l \in \{l = (i, j) : d_1(i, j) > 0\}. \quad (43)$$

Also, we are looking for stable solutions of the system and therefore the coefficients of exponentials with positive exponents must be set to zero. Since the eigenvalues  $\nu_m$  are either zero or negative, for stability it must be true that

$$\forall \sigma \in \{\sigma : r_{\sigma} > 0\}, \quad \bar{c}_{\sigma} = 0. \quad (44)$$

By solving the system of equations (43) and (44) we extract the coefficients  $\bar{c}_\sigma$ .

## II. Finite buffer case

At  $x_1 = 0$  the condition (43) remains. At  $x_1 = B$  the following condition is used:

$$\begin{aligned} & \Pr\{l = (i, j) \in U_2, x_1 \leq B, X_2 = 0\} + \Pr\{l = (l, j) \in U_2, \text{queue 1 full}, X_2 = 0\} = \\ & \Pr\{S(t) = l = (i, j) \in U_2, X_2 = 0\}. \end{aligned} \quad (45)$$

For source states that belong in the underflow set of source 1, queue 1 cannot be full, except at isolated time instances, and using our previous definitions we obtain,

$$\forall l \in \{l = (i, j) : d_1(i, j) < 0\}, \quad F_l^{10}(x_1 = B) = F_l^W(x_2 = 0). \quad (46)$$

By solving the system formed by the two conditions (that include as many equations as the number system states in  $U_1$ , which is also the number of unknown coefficients), the coefficients  $\bar{c}_\sigma$  can be derived for the finite buffer case. This completes the derivation of  $\mathbf{F}^{10}(x_1)$ , for both infinite and finite buffer cases. Similarly we can obtain  $\mathbf{F}^{20}(x_2) \stackrel{\text{def}}{=} \mathbf{F}(X_2 \leq x_2, X_1 = 0)$ . In the next section we describe the derivation of  $\mathbf{F}^{12}(x_1) \stackrel{\text{def}}{=} \mathbf{F}(X_1 \leq x_1, X_2 > 0)$  and the symmetrically defined  $\mathbf{F}^{21}(x_2)$ .

### 3.4 Derivation of Distribution $\mathbf{F}^{12}(x_1)$

We begin again by setting up the difference equations for the area  $0 \leq x_1$ , for the case that  $X_2(t) > 0$ . In this case, all source states  $S(t) \in \mathcal{G}$  are included. In this case there is no excitation to the system and the general solution can be easily obtained. If we set up the system equations we get the system in the following matrix form:

$$\mathbf{D}_2 \frac{d}{dx_1} \mathbf{F}^{12}(x_1) = \mathbf{G} \mathbf{F}^{12}(x_1), \quad (47)$$

where, the elements of the diagonal drift matrix  $\mathbf{D}_2$  are given by,

$$D(i, j) = \lambda_k - c_1, \quad k = (i, j) \in \mathcal{G}, \quad (48)$$

and  $\mathbf{G}$  is the global source generator, which was previously obtained. The general solution of  $F_i^{12}$  is,

$$F_i = \sum_l s_{il} k_l e^{z_l x_1}, \quad (49)$$

where  $s_{il}$  is the  $i$ th component of the  $l$ th eigenvector of  $\mathbf{D}_2^{-1} \mathbf{G}$ ,  $z_l$  is the corresponding eigenvalue, and the coefficients  $k_l$  are to be determined by boundary conditions.

### 3.5 Boundary conditions for $\mathbf{F}^{12}(x_1)$

#### I. Infinite buffer case

In (49) the unknown coefficients  $k_l$  can be determined by a linear system of equations that results by applying conditions at the boundaries  $x_1 = 0$  and  $x_1 = \infty$ . There are conditions corresponding to overflow states at  $x_1 = 0$ , one condition corresponding to the zero eigenvalue that contains the results of  $F^{10}(x_1)$  at infinity, and conditions that correspond to the positive eigenvalues and impose stability to the system solution.

At the point  $x_1 = 0$ , for all states such that the drift  $d_1(i, j)$  is positive, i.e., for all overflow states, the probability of empty queue 1 becomes zero:

$$F_k^{12}(x_1 = 0) = 0, \forall k \in \{k = (i, j) : d_1(i, j) > 0\}. \quad (50)$$

Also, to have stable system solutions, we must set the coefficients of exponential terms with positive exponents equal to zero, i.e.,  $k_l = 0$ , for  $l$  such that  $z_l = 0$ . Additionally, the term in the solution that contains the zero eigenvalue is given by

$$\begin{aligned} F_l^{12}(\infty) &= P_l(X_1 \leq \infty, X_2 > 0) \\ &= \pi_{1l} - P_l(X_1 \leq \infty, X_2 = 0) \\ &= \pi_{1l} - F_l^{10}(\infty), \end{aligned} \quad (51)$$

where  $l = (i, j) \in \mathcal{G}$ ,  $\pi_l$  is the known global source distribution at state  $l = (i, j)$ , and  $F_l^{10}(\infty)$  can be found by taking the limit  $\lim_{x_1 \rightarrow \infty}$  in the solution of  $F_l^{10}(x_1)$ . By solving the system of (50),(51) we can determine the coefficients  $k_l$  in (49), which completes the solution of  $\mathbf{F}^{12}(x_1)$ .

#### II. Finite buffer case.

At  $x_1 = 0$  the condition (50) remains.

At  $x_1 = B$  the following condition is used:

$$\begin{aligned} &\Pr\{l = (i, j) \in \mathcal{G}, x_1 \leq B, X_2 > 0\} + \Pr\{l = (l, j) \in \mathcal{G}, \text{queue 1 full}, X_2 > 0\} = \\ &\Pr\{l = (i, j) \in \mathcal{G}, X_2 > 0\}. \end{aligned} \quad (52)$$

For source states that belong in the underflow set of source 1, queue 1 cannot be full, except at isolated time instances, and using our previous definitions we obtain,

$$\begin{aligned} \forall l \in \{l = (i, j) : d_1(i, j) < 0\}, \quad F_l^{12}(x_1 = B) &= P_l(X_2 > 0), \quad \text{or} \\ F_l^{12}(x_1 = B) &= \pi_l - F_l^{10}(x_1 = B). \end{aligned} \quad (53)$$

By solving the system formed by the two conditions (that include as many equations as the number system states in  $\mathcal{G}$ , which is also the number of unknown coefficients), the coefficients  $k_l$  can be derived for the finite buffer case. The distribution  $\mathbf{F}^{21}(x_2)$  can be derived similarly.

### 3.6 The Steady State Distributions and Performance Statistics

From the previous sections we have obtained  $\mathbf{F}_l^{10}(x_1)$ , and  $\mathbf{F}_l^{12}(x_1)$ . By applying the simple fact that

$$\Pr\{S(t) = l, X_1(t) \leq x_1\} = \Pr\{S(t) = l, X_1(t) \leq x_1, X_2(t) = 0\} + \Pr\{S(t) = l, X_1(t) \leq x_1, X_2(t) > 0\}, \quad (54)$$

as  $t \rightarrow \infty$  we get the steady state distribution  $\mathbf{F}(x_1)$ :

$$F_l(x_1) = F_l^{10}(x_1) + F_l^{12}(x_1), \forall l = (i, j) \in \mathcal{G}. \quad (55)$$

Similarly we can obtain the occupancy distribution of the second logical queue  $\mathbf{F}(x_2)$ .

Once the steady state distribution for the content of each session in the shared buffer is determined, it is possible to obtain expressions for their throughput and loss probabilities. Let  $F_k^Y(y)$  denote the steady state probability distribution function of the random variable  $Y = X_1 + X_2$ , at global system state  $k \in \mathcal{G}$ , i.e., the occupancy distribution of the total shared buffer content irrespective of priority class. In the following we assume known the exact method to derive  $F_k^Y(y)$ , given a general MMF input source, the total server capacity  $c$ , and a finite buffer of size  $B$  (see for example [12]). The throughput  $T_1$  of session 1 is given by the following expression:

$$T_1 = (\text{generation rate of session 1}) - (\text{loss rate of session 1}) \quad (56)$$

$$= \sum_{k \in \mathcal{G}} \pi_{1k} \lambda_k - \quad (57)$$

$$\sum_{k \in \mathcal{G}} \{[\lambda_k - c_1]^+ \Pr\{k, \text{buffer full}, X_2 > 0\} + [\lambda_k + \mu_k - c]^+ \Pr\{k, \text{buffer full}, X_2 = 0\}\} \quad (58)$$

$$= \sum_{k \in \mathcal{G}} \pi_{1k} \lambda_k - \quad (59)$$

$$\sum_{k \in \mathcal{G}} \{[\lambda_k - c_1]^+ [\Pr\{k, \text{buffer full}\} - \Pr\{k, X_1 = B\}] + [\lambda_k + \mu_k - c]^+ \Pr\{k, X_1 = B\}\}. \quad (60)$$

In this expression for  $T_1$  it is taken into account that the drift of session 1 depends on the content of session 2. It is known that  $\Pr\{k, \text{buffer full}\} = \pi_{1k} - F_k^Y(B)$  and  $\Pr\{k, X_1 = B\} = \pi_{1k} - F_k^{10}(B)$ . Substituting in the expression for  $T_1$  we obtain the throughput of session 1. The loss probability  $L_1$  of session 1 can then be simply derived as follows:

$$L_1 = 1 - \frac{T_1}{\sum_{k \in \mathcal{G}} \pi_{1k} \lambda_k}. \quad (61)$$

In conventional fluid analysis, the distribution for the waiting time is readily obtained from the distribution for the buffer content. However, in the model considered, this is not trivial since the

service rate for a given session depends on the content of the other session's logical queue. An estimate of the distribution of delay seen by arriving cells of session 1 is,

$$\Pr\{\text{delay} \leq t\} = \frac{1}{T_1} \sum_{k \in \mathcal{G}} \lambda_k F_k(X_1 \leq c_1 t), \quad 0 \leq t < B/c_1, \quad (62)$$

where we conservatively assume that the service rate of session 1 remains at its minimum guaranteed value  $c_1$  upon cell arrival. We note however that the occupancy distribution in (62) is derived from the previous analysis.

Similar expressions can be obtained for the throughput, loss probability and delay distribution of session 2.

## 4 Numerical Results

In order to verify the accuracy of our approximation we conducted numerical results to compare analysis with simulation for the tail distributions  $P_i[X_i > x_i]$ ,  $i = 1, 2$  of the two sessions. Results are included for both the infinite and finite shared buffer case. In all the simulation cases under study the simulation run lengths were such that the 95% confidence interval of an estimated value is within 20% of the value.

Although the analysis accounts for any number of multistate MMF sources in each of the two different priority traffic streams, we use two-state sources for simplicity. Each input traffic stream  $i$  consists of a two-state MMF source (on-off source) characterized by the state transition rates  $a_i$  and input rate  $\lambda_i$  (on state) for source 1, and  $b_i$  and input rate  $\mu_i$  (on state) for source 2. The average duration of the on state is kept equal to 1 in all cases, i.e.  $1/a_2 = 1/b_2 = 1$ . The total server capacity  $c = 1$ . The GPS assignment is symmetrical, i.e.,  $c_1 = c_2 = 0.5$ , in all but the last example. We are mostly interested in obtaining results when traffic load approaches critical levels. In figures (3) through (6) the overflow probability of both sessions is estimated and simulated with source activity factors  $\rho_1 = a_1/(a_1 + a_2)$ ,  $\rho_2 = b_1/(b_1 + b_2)$ , respectively, where  $\rho_1 = \rho_2 = 0.4$ . The on-state rates are  $\lambda_1 = \mu_1 = 1.01$ , that corresponds to total system load  $u = 0.8$  in all figures. Each graph corresponds to a different GPS assignment  $(c_1, c_2)$  which defines the fraction of the total service that each source receives. In fig. (3)  $c_1 = c_2 = 0.5$  the GPS assignment is symmetrical, while in the rest of the figures it is asymmetrical. Since the same sources are used in our examples, the effect of assigning a different fraction of service to each source on the buffer occupancy is more apparent. As more service is assigned to the first source the difference of the overflow probabilities of the two sources increases. Although this is a simple qualitative fact the analysis can help quantify this effect.

In figures (5) through (10) we used the same source parameter values with various GPS as-



signments, this time for the case of a finite buffer with  $B = 10$ . To give some numerical intuition we may equate the server capacity of one fluid unit per time unit to the standard OC-3 rate of 155 Mbps. By using a time unit of 0.27 msec, one unit of fluid then corresponds to 100 ATM cells, so  $B = 10$  is equivalent to 1000 cells. In both cases the analytical results are higher than the simulation results. Although this is not proven in general, it is intuitively expected since in the first step of the analysis we assume independence of the two queue occupancy distributions in order to obtain the excitation of the system equations on both the  $x_1$  and  $x_2$  axis. We intend to investigate whether iterating on the values of the occupancy distributions in area W, using the results for  $\mathbf{F}(x_1)$ ,  $\mathbf{F}(x_2)$  refines our approximation, as we expect.

#### 4.1 A Comparative Study with a Fixed Capacity Allocation System

Using our analysis we can explicitly demonstrate the significant improvement in resource allocation during admission control when using capacity scheduling with the GPS policy and shared buffering, as compared to a segregated buffer system with fixed capacity assignment for each priority class. We assume a scenario in which each source of the previous examples belongs to a traffic class with different loss requirements,  $L_1 = 10^{-6}$  and  $L_2 = 10^{-3}$ . We then examine the minimum capacity that satisfies the loss requirement for a wide range of buffer sizes in two buffer management systems. In the first system each traffic stream  $i$  uses a dedicated buffer of size  $B_i$  and capacity  $C_i$ . To obtain the optimal capacity allocation for each overall system buffer size  $B$ , we solve the minimization problem:

$$\begin{aligned} & \text{Minimize } f(C_1, C_2) = C_1 + C_2 \\ & \text{Subject to: } L_1(C_1, B_1) = 10^{-6}, L_2(C_2, B_2) = 10^{-3}, \\ & \text{and } B_1 + B_2 = B. \end{aligned}$$

For each value of  $B$  the optimization procedure finds the optimal buffer partitioning  $(B_1, B_2)$  that minimizes the overall capacity  $C$ .

In the second system we use GPS scheduling with assignment  $(c_1, c_2)$  and complete sharing of a buffer of size  $B$ . For each overall system buffer size  $B$  we solve the minimization problem:

$$\begin{aligned} & \text{Minimize } f(C) = c_1 C + c_2 C = C \\ & \text{Subject to: } L_1(C_1 = c_1 C, B) = 10^{-6}, L_2(C_2 = c_2 C, B) = 10^{-3}, \\ & \text{and } c_1 + c_2 = 1. \end{aligned}$$

In this case the optimization procedure finds the minimum required capacity  $C$  as well as the optimal GPS assignment  $(c_1, c_2)$ . Comparative numerical results were obtained using Matlab library functions for optimization and are illustrated in fig. (11). There are two optimal capacity-buffer curves for fixed losses  $L_1$  and  $L_2$ , one for the segregated buffer/capacity system, and one for the complete buffer sharing GPS system.

In both cases, as the buffer size increases less capacity is required to meet the loss requirements of the two priority classes. For all buffer sizes the shared buffer GPS system requires less capacity. Specifically, for buffer sizes from 500 to 2500 cells ( $B = 5$  to 25) savings in capacity range from 70% to 10%. This is a region of typical buffer sizes of interest, roughly covering the first quarter of the  $x_1$ -axis in fig. (11). Observe also that in this region the optimal curves are much steeper. However the slope of the shared GPS system is smaller, which means that by reducing the available capacity by some amount, much less additional buffer is needed for the shared GPS system to meet the loss requirement, than in the segregated system. Alternatively, for any available capacity the shared buffer GPS system can meet the loss requirements using a smaller buffer size. This is a tradeoff that is useful in buffer sizing. The shared GPS system optimal curve also provides a means to compare how different implementations of packetized GPS approach the continuous fluid analysis performance.

## 5 Conclusions

In this paper, we studied the performance of sharing buffer space and link capacity between two sessions, the traffic of which is modeled by two independent general MMF sources. For scheduling we assumed the GPS policy, which guarantees a minimum capacity allocation to each session, and thus allows for maintaining different quality of service, in terms of loss probability and delay. Among admission policies assigning buffer space priority when the shared buffer is full, we focus on complete buffer sharing. At a first step, our analytical approach obtains estimates that approximate the occupancy distribution for the logical queue of each session. At a second step we obtain refined estimates of the occupancy distributions by first obtaining expressions for the constrained distributions on and inside the boundaries. Moreover, we obtain analytical results for the throughput, loss probability and delay distribution. Case studies in traffic loads of interest show that the analytical results closely approximate the results obtained by simulations and give upper bounds. Although in this paper we focused on complete sharing of the buffer, the techniques used can be extended to model other space priority policies that control access to the buffer when it is full, such as push-out, combined with GPS scheduling. This class of mixed buffer space and capacity policies conserve the network resources, and allow for flexibility in assigning loss and delay priorities among different traffic classes.

Finally, we compared the optimal capacity allocation for a wide range of buffer sizes, between the system under analysis and a fixed capacity assignment segregated buffer multiplexer with the same total buffer size. We observed considerable gain in the required capacity in the buffer size regions of interest. Common call admission control methods assume a fixed effective capacity (or bandwidth) allocation for the sake of its additive property and call set-up speed. Our results indicate that there can be significant improvement in the capacity allocation to calls, by further exploiting the multiplexing gain of shared buffers and GPS scheduling. Similar performance trends are expected when more than two priority classes are present, which still remains an interesting direction for future research.

## References

- [1] A.K. Parekh and R.G. Gallager, "A Generalized Processor Sharing approach to flow control in Integrated Services Networks: the single node case," *IEEE/ACM Trans. on Networking*, Vol. 1, No. 3, pp. 344-375, June 1993.
- [2] A.K. Parekh and R.G. Gallager, "A Generalized Processor Sharing approach to flow control in Integrated Services Networks: the multiple node case," *Proc. IEEE Infocom '93*, pp. 521-530, 1993.
- [3] R. L. Cruz, "A calculus for network delay, part I: network elements in isolation," *IEEE Trans. on Inform. Theory*, Vol. 37, No. 1, pp. 114-131, Jan, 1991.
- [4] O. Yaron and M. Sidi, "Generalized Processor Sharing networks with Exponentially Bounded Burstiness Arrivals," *Proc. IEEE Infocom '94*, pp. 628-634, June 1994.
- [5] Z.-L. Zhang, D. Towsley, and J. Kurose, "Statistical analysis of Generalized Processor Sharing Scheduling Discipline." *IEEE J. on Sel. Areas in Comm.*, Vol. 13, No. 6, pp. 1-10, Aug. 1995.
- [6] O. Yaron and M. Sidi, "Performance and stability of communication networks via robust exponential bounds," *IEEE/ACM Trans, on Networking*, Vol. 1, No. 3, pp. 372-385, 1993.
- [7] F. Lo Presti, Z.-L. Zhang, and D. Towsley, "Bounds, Approximations and applications for a two-queue GPS system," *Proc. IEEE Infocom '96*, Vol. 3, pp. 1310-1317, 1996.
- [8] A. I. Elwalid, D. Heyman, T. V. Lakshman, D. Mitra, and A. Weiss, "Fundamental bounds and approximations for ATM multiplexers with applications to video teleconferencing," *IEEE J. Select. Areas Commun.*, Vol. 13, No. 6, pp. 1004-1016, Aug. 1995.
- [9] Guo-Liang Wu and Jon W. Mark, "A buffer allocation scheme for ATM Networks: Complete sharing based on virtual partition," *IEEE/ACM Trans. on Networking*, Vol. 3, No. 6, Dec. 1995.

- [10] D. Anick, D. Mitra, and M. M. Sondhi, "Stochastic theory of a data-handling system with multiple sources," *The Bell Syst. Tech. J.*, Vol. 61, No. 8, Oct. 1982.
- [11] A. Elwalid, and D. Mitra, "Analysis and design of rate-based congestion control of high-speed networks, I: stochastic flow models, access regulation," *Queueing Systems*, Vol. 9, pp. 29-64, 1993.
- [12] Roger F. Tucker, "Accurate method for analysis of a packet-speech multiplexer with limited delay," *IEEE Trans. on Commun.*, Vol. 36, No. 4, April 1988.
- [13] A. T. Andersen and B. F. Nielsen, "An application of superpositions of two state Markovian sources to the modelling of self-similar behavior," *Proc. IEEE Infocom '97*, 1997.
- [14] Harry G. Peros and Khaled M. Elsayed "Call Admission Control Schemes: A Review ," *IEEE Commun. Mag.*, Vol. 34, No. 11, November 1997.

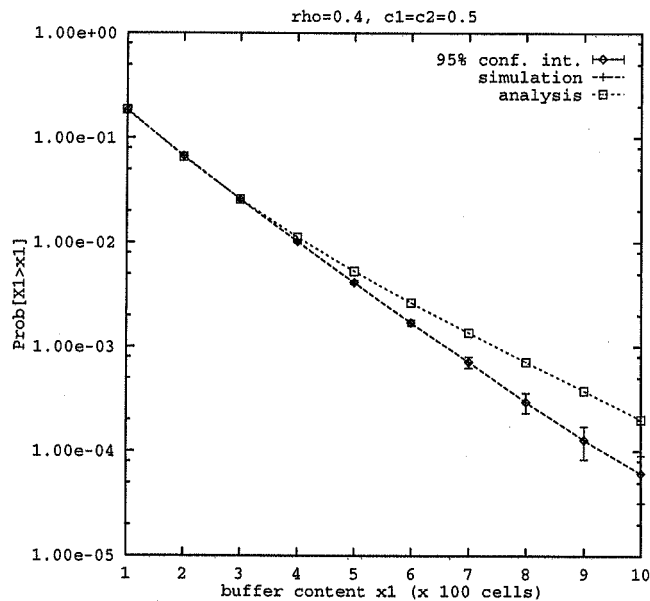


Figure 3: Tail distribution of sessions 1 and 2 in the infinite buffer case, GPS assignment  $c_1 = c_2 = 0.5$

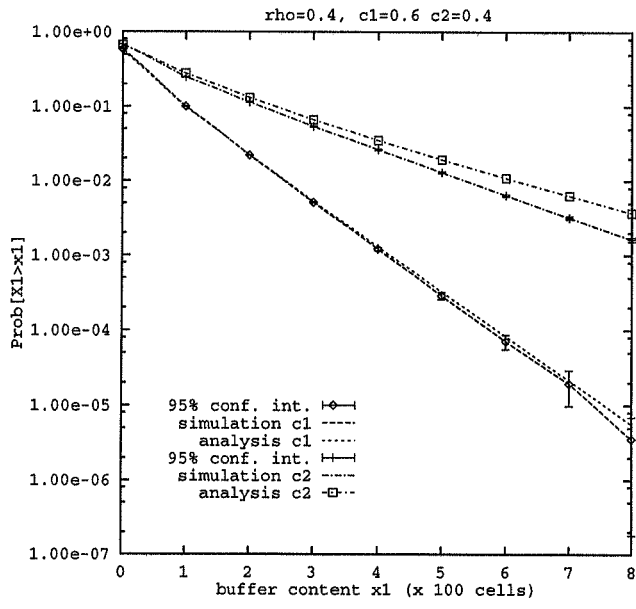


Figure 4: Tail distribution of sessions 1 and 2 in the infinite buffer case, GPS assignment  $c_1 = 0.6, c_2 = 0.4$

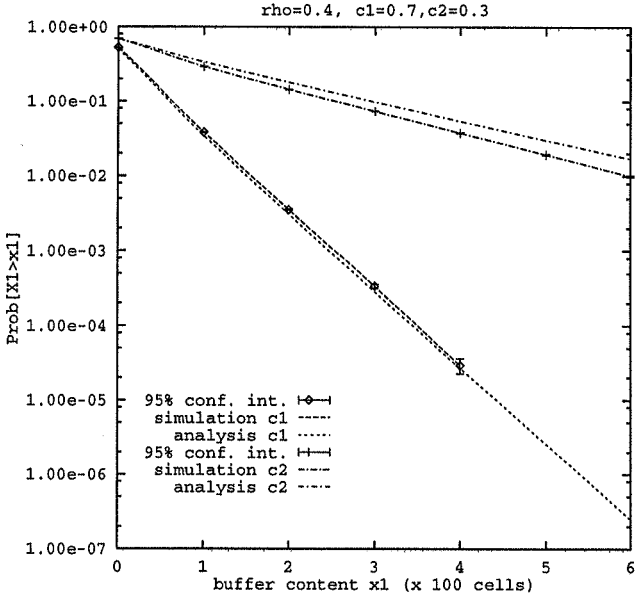


Figure 5: Tail distribution of sessions 1 and 2 in the infinite buffer case, GPS assignment  $c_1 = 0.7, c_2 = 0.3$

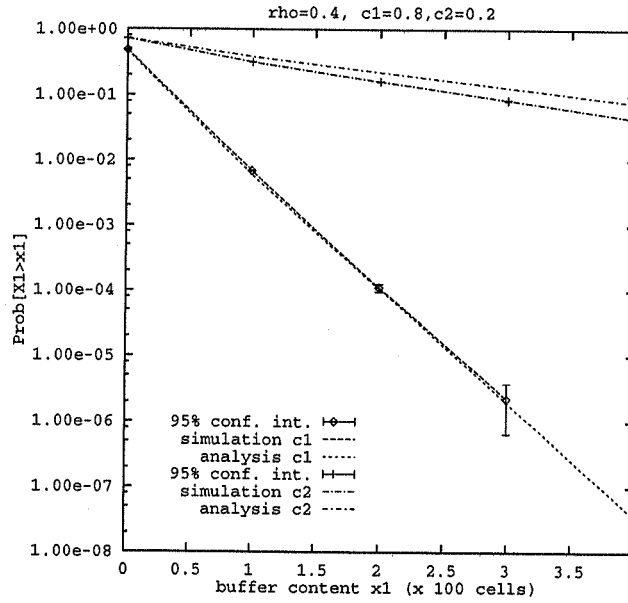


Figure 6: Tail distribution of sessions 1 and 2 in the infinite buffer case, GPS assignment  $c_1 = 0.8$ ,  $c_2 = 0.2$

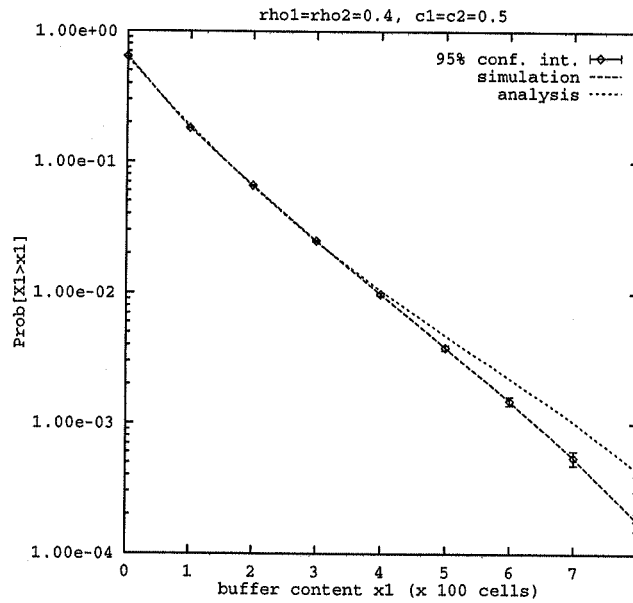


Figure 7: Tail distribution of sessions 1 and 2, with finite shared buffer  $B = 10$ , GPS assignment  $c_1 = c_2 = 0.5$

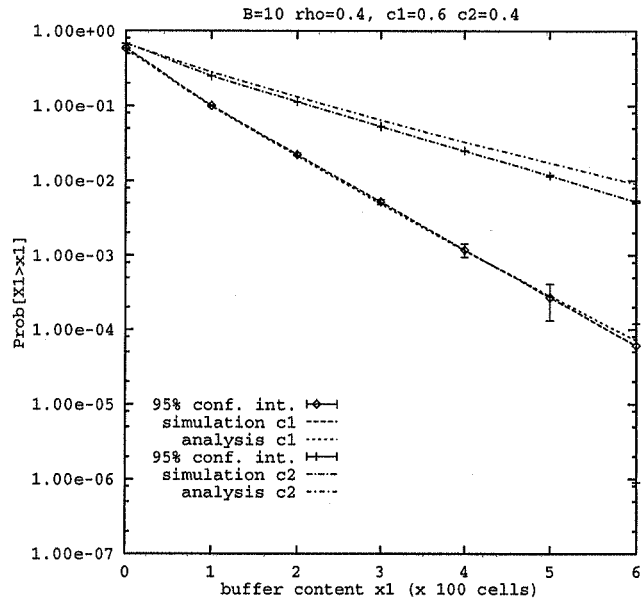


Figure 8: Tail distribution of sessions 1 and 2, with finite shared buffer  $B = 10$ , GPS assignment  $c_1 = 0.6, c_2 = 0.4$

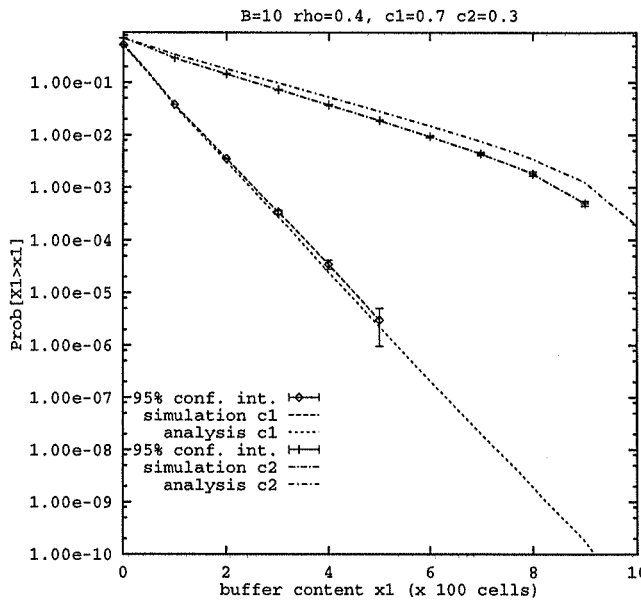


Figure 9: Tail distribution of sessions 1 and 2, with finite shared buffer  $B = 10$ , GPS assignment  $c_1 = 0.7, c_2 = 0.3$

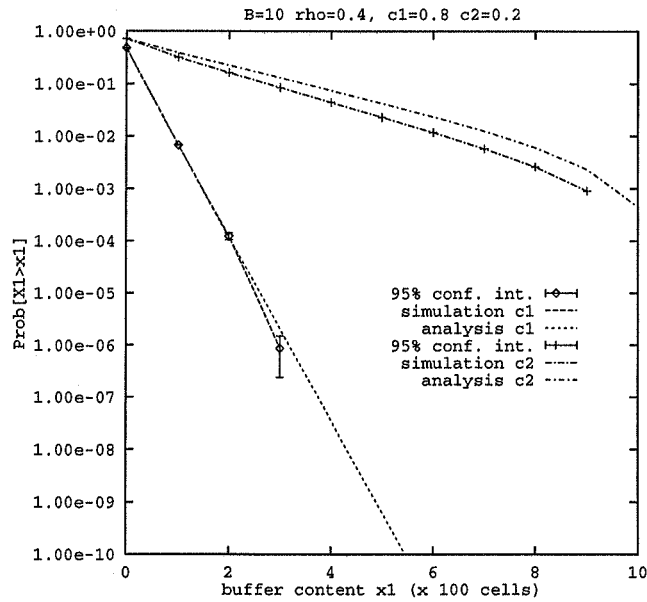


Figure 10: Tail distribution of sessions 1 and 2, with finite shared buffer  $B = 10$ , GPS assignment  $c_1 = 0.8, c_2 = 0.2$

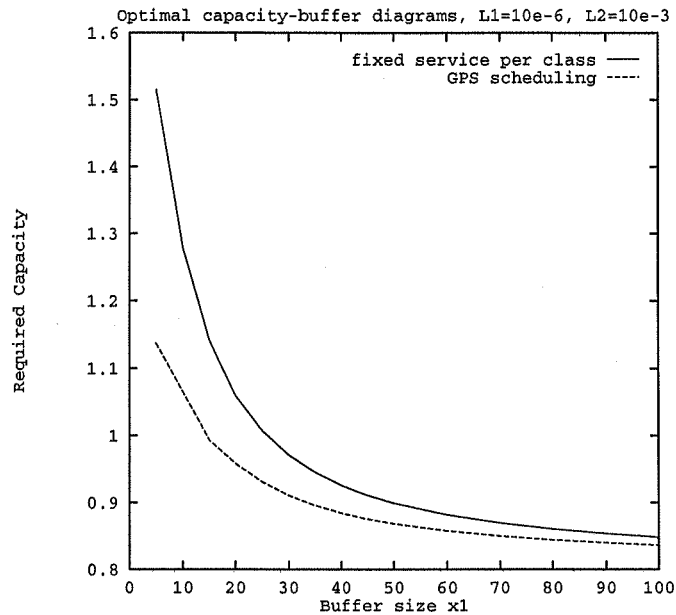


Figure 11: Comparison of the shared buffer GPS system with a segregated buffer fixed capacity allocation system of the same total buffer size.